



Published as: *J Immunol.* 2015 March 1; 194(5): 2260–2267.

## Dermal resident versus recruited $\gamma\delta$ T cell response to cutaneous Vaccinia virus infection

Amanda S. Woodward Davis<sup>\*</sup>, Tessa Bergsbaken<sup>\*,†</sup>, Martha A. Delaney<sup>‡</sup>, and Michael J. Bevan<sup>\*,†</sup>

<sup>\*</sup>Department of Immunology, University of Washington, Seattle, WA 98109

<sup>†</sup>Howard Hughes Medical Institute, University of Washington, Seattle, WA 98109

<sup>‡</sup>Department of Comparative Medicine, University of Washington, Seattle, WA 98109

### Abstract

The study of T cell immunity at barrier surfaces has largely focused on T cells bearing the  $\alpha\beta$  T cell receptor. However, T cells that express the  $\gamma\delta$  T cell receptor are disproportionately represented in peripheral tissues of mice and humans, suggesting they too may play an important role responding to external stimuli. Here we report that in a murine model of cutaneous infection with Vaccinia Virus, dermal  $\gamma\delta$  T cell numbers increased ten-fold in the infected ear and resulted in a novel  $\gamma\delta$  T cell population not found in naïve skin. Circulating  $\gamma\delta$  T cells were specifically recruited to the site of inflammation and differentially contributed to dermal populations based on their CD27 expression. Recruited  $\gamma\delta$  T cells, the majority of which were CD27<sup>+</sup>, were Granzyme B<sup>+</sup> and made up about half of the dermal population at the peak of the response. In contrast, recruited and resident  $\gamma\delta$  T cell populations that made IL-17 were CD27<sup>-</sup>. Using a double chimera model that can discriminate between the resident dermal and recruited  $\gamma\delta$  T cell populations, we demonstrated their divergent functions and contributions to early stages of tissue inflammation. Specifically, the loss of the perinatal thymus-derived resident dermal population resulted in decreased cellularity and collateral damage in the tissue during viral infection. These findings have important implications for our understanding of immune coordination at barrier surfaces and the contribution of innate-like lymphocytes on the front lines of immune defense.

### INTRODUCTION

The skin is host to a network of T lymphocytes, some of which take up permanent residence within the tissue, having been recruited there throughout life, while others are only transiently present (1, 2). Following antigen-specific activation in central lymphoid organs, TCR $\alpha\beta$  effector cells traffic to peripheral sites, including the skin, and some become resident memory T cells (T<sub>RM</sub>). These cells are recruited into the tissue as a result of local infection or inflammatory signals and remain there to protect against future external insults (3–8). In contrast to TCR $\alpha\beta$  T<sub>RM</sub> cells, TCR $\gamma\delta$  T cells have been shown to home to tissues and acquire specific functions as a result of developmental programming and their response

Address correspondence and reprint requests to Michael J. Bevan, Department of Immunology, University of Washington, Box 358059, 750 Republican St, Seattle, WA 98109. mbevan@uw.edu.

via TCR recognition of foreign antigens in poorly defined (9–11). This hardwiring, which drives them particularly to barrier tissues such as the intestine, reproductive tract and skin, seems ideally suited to ensure that  $\gamma\delta$  T cells participate in innate host defense.

Within the murine skin, dendritic epidermal T cells (DETC) are resident in the epidermis. They seed the skin during fetal development, express an invariant V $\gamma$ 5 TCR, have dendritic morphology and are relatively immobile (12). They have been shown to participate in keratinocyte maintenance, to respond to wounding, and to assist in the healing process (13–15). A different subset of TCR $\gamma\delta$  T cells are resident in the dermis. Dermal  $\gamma\delta$  T cells comprise up to half of the dermal T cells in mice (16) and 2–9% in humans (17). This population has been shown to participate in host defense against bacterial infection of the skin (16, 18) as well as to contribute to psoriasis in the mouse (19, 20) and humans (21). It is now appreciated that in mice, dermal  $\gamma\delta$  T cells exit the thymus and seed the dermis near the time of birth (11, 22). Characterization of dermal  $\gamma\delta$  T cells by several groups has revealed their memory phenotype and functions related to that of CD4<sup>+</sup> T<sub>H</sub>17 cells, being capable of producing IL-17 upon stimulation *in vitro*. Dermal  $\gamma\delta$  T cells express CCR6, CXCR6, CD103, CD44, IL-23R and IL-7R (21–23). However, it is unclear whether IL-17-producing dermal  $\gamma\delta$  T cell populations observed during infection or inflammation are derived from the resident population seeded there at birth or if unique populations are recruited from the circulation.

A recent study identified a population of  $\gamma\delta$  T cells that is enriched in skin draining lymph nodes (dLN) of mice with properties similar to those of dermal  $\gamma\delta$  T cells (22). This discovery demonstrated a potential link between dermal  $\gamma\delta$  T cells and those found in the circulation. While several models of systemic viral infection (24, 25) have elicited a  $\gamma\delta$  T cell response in the spleen and LN, these studies did not address questions concerning tissue trafficking or provide a relevant context for natural modes of infection. Importantly, studies with human PBMC have found that  $\gamma\delta$  T cells in the circulation are impacted in patients with inflammatory bowel disease (26), melanoma (27) and psoriasis (28), suggesting that local inflammation can impact global  $\gamma\delta$  T cell homeostasis. These findings point to the need to understand the trafficking patterns of  $\gamma\delta$  T cells during steady state conditions and in the context of disease.

Emerging data from studies of cells in central lymphoid organs suggest that CD27 delineates  $\gamma\delta$  T cell functional subsets, leading to a paradigm shift for how  $\gamma\delta$  T cells are classified (11, 29). Expression of CD27 by mouse  $\gamma\delta$  T cells is tightly correlated with their ability to produce IFN $\gamma$ , where failure to express CD27 correlates with IL-17 production (30). Importantly, analogous  $\gamma\delta$  T cell populations have been found in human PBMC (31–33), making this a relevant axis from which to orient experiments in model organisms.

In the current study, we analyzed the  $\gamma\delta$  T cell response in mouse skin to local infection with Vaccinia Virus (VV). We sought to dissect the contribution of resident versus immigrant  $\gamma\delta$  T cells following infection and to determine whether  $\gamma\delta$  T cells recruited from the circulation give rise to long-term residents in the skin after the cutaneous infection has cleared. Many previous reports have studied the  $\gamma\delta$  T cell response in TCR $\alpha^{-/-}$  or TCR $\beta^{-/-}$  mice which lack TCR $\alpha\beta$  T cells (24, 25) or performed transfers of  $\gamma\delta$  T cells isolated from TCR $\beta^{-/-}$  mice

(34) to investigate the anti-viral response. In such scenarios the  $\gamma\delta$  T cell makeup and response is likely abnormal (35). Analyzing  $\gamma\delta$  T cells in a wild-type setting allowed us to better appreciate their role in a skin infection. Our experiments revealed that CD27<sup>+</sup> and CD27<sup>-</sup>  $\gamma\delta$  T cells are specifically recruited from the circulation to the site of infection, but surprisingly do not become resident in the tissue, even when encountering a relatively empty niche. The immigrant  $\gamma\delta$  T cells have functional attributes distinct from the resident dermal  $\gamma\delta$  T cells, the latter being primarily responsible for enhancing the inflammatory response in the tissue.

## METHODS

### Mice

C57BL/6, B6.SJL-Ptprc<sup>a</sup> Pepc<sup>b</sup>/BoyJ and TCR $\delta^{-/-}$  mice were obtained from the Jackson Laboratory and TCR $\delta$ -H2BeGFP (TCR $\delta$ -GFP) mice were obtained from I. Prinz (Hannover Medical School) and have been described previously (36). Mice were housed in specific pathogen-free conditions in the animal facilities at the University of Washington and unless otherwise specified were used at 6–10 weeks of age. All experiments were done in accordance with the Institutional Animal Care and Use Committee guidelines of the University of Washington.

### Infections

$2 \times 10^6$  plaque forming units (PFU) of recombinant Vaccinia Virus expressing full-length chicken ovalbumin (VV-OVA) was used for epicutaneous infection by skin scarification, as described previously (37). Mice were anesthetized with isoflurane and 5  $\mu$ l of diluted virus was applied to the dorsal side of the ear. The skin area was then gently scratched 20 times with a 28-gauge needle. For flow cytometry experiments, both ears of mice were infected and combined to comprise one sample and the numbers were divided by two to obtain the number of cells/ear.

### Adoptive transfer and sorting

C57BL/6 or CD45.2<sup>+</sup> TCR $\delta$ -GFP mice received  $7 \times 10^5$   $\gamma\delta$  T cells enriched from spleen and skin dLN of CD45.1<sup>+</sup> TCR $\delta$ -GFP mice by i.v. injection one day before infection. Enrichment of  $\gamma\delta$  T cells was performed by incubating single cell suspensions with biotin-labeled anti-TCR $\beta$  and anti-CD19 mAb for 30 minutes on ice, followed by passage through the Stem Cell Biotin negative selection kit. Mice were infected on one ear and the infected (or uninfected) ears from two mice were combined for each sample. In some experiments, the enriched population was further purified as follows: cells were stained with fluorochrome-conjugated anti-CD27 and sorted on a FACS Aria for the GFP<sup>+</sup>TCR $\beta^{-}$ CD19<sup>-</sup>CD27<sup>+</sup> or GFP<sup>+</sup>TCR $\beta^{-}$ CD19<sup>-</sup>CD27<sup>-</sup> populations, of which >97% were TCR $\gamma\delta^{+}$ .  $6 \times 10^5$  CD27<sup>+</sup> or  $2.7 \times 10^5$  CD27<sup>-</sup> sorted  $\gamma\delta$  T cells from B6.SJL-Ptprc<sup>a</sup> Pepc<sup>b</sup>/BoyJ (CD45.1) mice were transferred into separate C57BL/6 (CD45.2) hosts. Mice that received sorted cells were infected on both ears and ears from a single mouse were combined for a sample.

## Flow Cytometry

Single cell suspensions were prepared from spleens and LN by mechanical disruption. Dorsal and ventral halves of ears were separated, minced and then enzymatically digested for 2 hrs at 37 °C in Liberase TM (Roche). Both ears from each mouse were combined for processing to obtain adequate cell numbers. All tissues were passaged through a 100- $\mu$ m nylon sieve (BD Bioscience). In some experiments, to avoid the Liberase digestion (which cleaved CD27), dorsal and ventral halves of the ears were separated and floated dermal side down in complete media overnight at 37°C. Supernatant, into which cells had migrated, was collected the following day and stained. Cells were stained for 30 min on ice with the appropriate mixture of monoclonal antibodies and washed with PBS containing 1% BSA. The following conjugated mAb were obtained from BD Pharmingen, eBioscience or BioLegend: anti- TCR $\beta$  (H57–597), CCR6 (140706), CD27 (LG.3A10), CD103 (2E7), V $\gamma$ 5 (BioLegend V $\gamma$ 3 clone 536), CD44 (IM7), CD45.1 (A20), CD45.2 (104). In the ear,  $\gamma\delta$  T cells from TCR $\delta$ -GFP were identified as GFP<sup>+</sup>V $\gamma$ 5<sup>-</sup> (dermal) or GFP<sup>+</sup>V $\gamma$ 5<sup>+</sup> (DETC), according to the nomenclature described by Heilig & Tonegawa (38). For the analysis of intracellular IFN $\gamma$ , IL-17 and Granzyme B, single cell suspensions were incubated in the presence or absence of 50 ng/mL PMA and 500 ng/mL Ionomycin for 4 hours at 37°C in the presence of Brefeldin A. Cells were stained for surface markers and then processed using the BD PharMingen Cytotfix/Cytoperm kit. Samples were analyzed on a FACSCanto II (BD) using Flowjo software (Tree Star).

## In situ proliferation

Infected mice were injected i.p. with 2mg in 200 $\mu$ l 50-Bromo-2-deoxyuridine (BrdU) 1 hour before being euthanized. Single cell suspensions were obtained from each tissue and stained using the BD Biosciences APC BrdU Kit. Cells were fixed with PFA before Cytotfix/Cytoperm to ensure retention of TCR $\delta$ -GFP signal.

## Bone marrow chimeras

Chimeras were made as previously described (22). Briefly, perinatal thymocytes (pThy) were harvested 0–48 h after birth and  $5 \times 10^6$  cells were transferred i.v. to congenic recipients that had been lethally irradiated with a dose of 1000 rad in a cesium irradiator. The next day,  $1-2 \times 10^6$  congenic bone marrow (BM) cells were transferred. These mice are referred to as “BMpThy chimeras” while controls without pThy are referred to as “BM chimeras”. Chimeras were analyzed or infected at least 8 weeks after reconstitution.

## Virus titration

The viral load in organs was determined by plaque assays on 143B cells with dilutions of a 40% tissue homogenate added to confluent wells. Titters reported are log<sub>10</sub> PFU per whole LN or ear.

## Histology

Ears from infected mice were fixed in 10% buffered formalin for 3 days before being embedded vertically in paraffin. Sections were hematoxylin and eosin stained and the

severity of inflammation and necrosis was determined on a scale of 0–4 (4 being the most severe). Scoring of all samples was blinded and uninfected mice were used as controls.

### Statistical analysis

Prism software (GraphPad) was used for all statistical analysis. The two-tailed, unpaired student *t*-test was used for comparisons of  $\gamma\delta$  T cell frequencies and histological scores.

## RESULTS

### $\gamma\delta$ T cells accumulate at the site of infection with the emergence of a novel dermal population

Although it is known that  $\gamma\delta$  T cells reside at barrier surfaces in mice and humans (16, 17), few studies have addressed the role they play during infection of the skin, particularly in response to viral infection. To address this, we used a model of Vaccinia Virus (VV) scarification, in which virus localizes primarily to the site of inoculation (39). Following infection of the ear pinna, we observed the number of dermal  $\gamma\delta$  T cells increased approximately ten-fold in the infected ear and dLN (Figure 1A & B). The response kinetics were slightly unusual, as the numbers in the skin and dLN remained elevated for a protracted period of time. Furthermore, the number of dermal  $\gamma\delta$  T cells at late time points was significantly higher than in naive ears, suggesting that infection could result in prolonged alterations in the dynamics of the dermal  $\gamma\delta$  T cell population. The number of DETC also increased about three-fold following infection and returned to the number found in control ears at late time points (Figure 1A).

Dermal  $\gamma\delta$  T cells have been reported to express CCR6 and CD103 (22). We confirmed that in resting skin, all dermal  $\gamma\delta$  T cells are CD103<sup>+</sup> and over half are CCR6<sup>+</sup> (Figure 1C & D). Skin scarification with VV resulted in dramatic changes in the dermal  $\gamma\delta$  T cell population. By three days post infection, a novel subset appeared in the dermis that was CCR6 and CD103 double negative (DN). This novel dermal  $\gamma\delta$  T cell subset accounted for almost half of the  $\gamma\delta$  T cell population at the peak of the response, then disappeared entirely from the dermis by 30 days post infection (Figure 1C & D). We also assessed TCR V $\gamma$  chain expression using commercially available antibodies on the three dermal populations and found they were all similarly heterogeneous (data not shown).

### Circulating $\gamma\delta$ T cells are rapidly recruited to the VV infected ear

We performed an adoptive transfer to investigate the origin of the dermal  $\gamma\delta$  T cell populations following infection and to determine the contribution of circulating  $\gamma\delta$  T cells to the expanded dermal population. Accordingly,  $7 \times 10^5$   $\gamma\delta$  T cells isolated from the spleen and skin dLN of naïve TCR $\delta$ -GFP mice were transferred intravenously into normal C57BL/6 recipients before VV scarification. Infection of the recipients showed that donor  $\gamma\delta$  T cells were specifically recruited to the skin of the infected ear and their numbers peaked 7 days post infection (Figure 2A). While these adoptively transferred, circulating cells were capable of entering the dermis during active infection, very few remained permanently integrated into the dermis at a late time point.

In the peripheral lymphoid organs and the circulation, it has been established that  $\gamma\delta$  T cells can be functionally segregated based on CD27 expression (11, 29). We found that CD27 and CCR6 staining were mutually exclusive in peripheral lymphoid organs and identified three  $\gamma\delta$  T cell populations with distinct surface and transcription factor staining patterns (Figure 2B & Supplemental Figure 1A). In line with previous reports that CD27<sup>-</sup>  $\gamma\delta$  T cells produce IL-17 upon stimulation, we found that baseline expression of the transcription factor ROR $\gamma$ t was higher in CD27<sup>-</sup> than in CD27<sup>+</sup>  $\gamma\delta$  T cells. Conversely, the transcription factor Tbet was highest in the CD27<sup>+</sup>  $\gamma\delta$  T cells. CCR6<sup>+</sup>CD27<sup>-</sup>  $\gamma\delta$  T cells expressed the highest levels of CD44 and CD103, while the small number of CD27<sup>-</sup>CCR6<sup>-</sup> cells and the CD27<sup>+</sup> cell subset had lower levels of CD44 and only half expressed CD103.

Transfer experiments revealed that the donor  $\gamma\delta$  T cells contributed to all three dermal  $\gamma\delta$  T cell populations defined by CD103 and CCR6 staining (Figure 2C), but it was not clear how these populations related to those in the circulation. Our initial attempts to stain for CD27 on  $\gamma\delta$  T cells isolated from the ear were negative. Further analysis revealed that CD27 was cleaved during the digestion process used to isolate cells from the ear. Floating ears (dorsal and ventral sides separated) overnight in complete media without enzymatic digestion released some  $\gamma\delta$  T cells from the tissue and permitted analysis of CD27 expression. This technique revealed that although CD27 was not found on dermal  $\gamma\delta$  T cells in naïve animals, it was expressed on some dermal  $\gamma\delta$  T cells following infection, all of which belonged to the CD103<sup>-</sup>CCR6<sup>-</sup> DN population (Supplemental Figure 1B). This suggested that the CD103<sup>-</sup>CCR6<sup>-</sup> DN subset appearing in infected ears was an immigrant population of circulating CD27<sup>+</sup>  $\gamma\delta$  T cells. Because yields and subset composition from the floating technique were variable, we opted to use CD103 and CCR6 for further analyses of skin samples.

To ask whether CD27<sup>+</sup> or CD27<sup>-</sup>  $\gamma\delta$  T cells from the circulating pool differentially contributed to the three dermal  $\gamma\delta$  T cell subsets, we sorted and transferred them into separate hosts before ear scarification with VV. The CD27<sup>-</sup> donor  $\gamma\delta$  T cells contributed to all three dermal populations defined by CD103 and CCR6, although few were DN and most expressed CD103 (Figure 2D). In contrast, immigrant  $\gamma\delta$  T cells from the CD27<sup>+</sup> donor population were exclusively CD103<sup>-</sup>CCR6<sup>-</sup> DN, even though 50% of cells in the donor population expressed CD103 (Supplemental Figure 1A). On a per cell basis, the CD27<sup>-</sup>  $\gamma\delta$  T cells were recruited more efficiently to the infected skin (data not shown). These experiments additionally demonstrate that *in vivo* in the presence of inflammatory signals, CD27 expression remains stable in the LN and spleen as a marker of distinct  $\gamma\delta$  T cell lineages. Based on these experiments and the fact that we observed very limited proliferation within the tissue (Supplemental Figure 2), it appears that the majority of  $\gamma\delta$  T cell accumulation is due to recruitment.

### Adult BM- and perinatal thymus-derived $\gamma\delta$ T cells occupy discrete niches

To tease apart the distinct roles of the resident dermal and circulating  $\gamma\delta$  T cell populations, we generated mice with and without resident dermal  $\gamma\delta$  T cells (22). We found that  $\gamma\delta$  T cells in the circulation and dermis were sensitive to whole body irradiation and that donor BM failed to reconstitute the dermal (Figure 3A) or the circulating CCR6<sup>+</sup>  $\gamma\delta$  T cell

populations (Supplemental Figure 3). The majority of the  $\gamma\delta$  T cells in the spleen and LN derived from the BM were  $CD27^+$  with a minority of  $CD27^-CCR6^-$   $\gamma\delta$  T cells. Although small numbers of host  $\gamma\delta$  T cells remained in the dermis following irradiation (Figure 3B), their phenotype was abnormal (data not shown) and their numbers were significantly lower than in unirradiated mice.

$\gamma\delta$  T cell populations lost due to irradiation were replaced by transferring perinatal thymocytes (pThy) into irradiated hosts along with congenically marked BM cells to generate mice referred to here as BMpThy chimeras. This resulted in the restoration of both dermal  $\gamma\delta$  T cells (Figure 3A & B) and the circulating  $CCR6^+$  population by pThy (Figure 3C). Total  $\gamma\delta$  T cell numbers in the dermis returned to normal levels and the phenotype of the pThy-derived dermal  $\gamma\delta$  T cells resembled that of unirradiated mice. Although pThy-derived  $\gamma\delta$  T cells contributed to all three circulating populations defined by  $CD27$  and  $CCR6$  staining,  $CD27^+$  cells were a relatively minor population, allowing us to generally discriminate between the resident dermal and recruited  $\gamma\delta$  T cell populations.

Using BMpThy chimeras, we confirmed that, following VV infection, adult BM-derived  $\gamma\delta$  T cells (largely  $CD27^+$  in the circulation) were transiently recruited from the circulation and contributed primarily to the  $CCR6^-CD103^-$  DN dermal subset (Figure 3D). In contrast, perinatal thymocyte-derived  $\gamma\delta$  T cells contributed mainly to the two  $CD103^+$  subsets in the dermis and their expansion during infection. As early as day 3 following infection, pThy-derived  $\gamma\delta$  T cells had expanded in the dermis and their numbers remained elevated for a protracted period of time. In contrast, the number of the BM-derived  $\gamma\delta$  T cells peaked at 7 days post infection and then declined dramatically. Importantly, at a late time point the BM-derived  $\gamma\delta$  T cells were absent from the ear while the pThy-derived  $\gamma\delta$  T cells plateaued at a level similar to wild type (WT) mice following infection.

### Adult BM- and pThy-derived $\gamma\delta$ T cells are functionally distinct

Several groups have established that dermal  $\gamma\delta$  T cells are fated to produce IL-17 (16, 21, 40). We found that a fraction of dermal  $\gamma\delta$  T cells in uninfected ears produced this cytokine following *in vitro* stimulation with PMA/Ionomycin. On day 3 after VV scarification,  $CD103^+$   $\gamma\delta$  T cells in the dermis were capable of producing IL-17 at a level similar to that of naïve tissue (Figure 4A). Although at any given time point the majority of IL-17 production was by  $CD103^+$   $\gamma\delta$  T cells (Supplemental Figure 4A), it was surprising that  $CD103^-$   $\gamma\delta$  T cells also produced IL-17 in the dermis. Using the float method in order to preserve  $CD27$  expression, we found that all the IL-17 production was by  $CD27^-$   $\gamma\delta$  T cells (Supplemental Figure 4B), which we predict are derived from the circulating  $CCR6^-CD27^-$  population (Figure 2C). Notably, there were no Granzyme B<sup>+</sup>  $\gamma\delta$  T cells in the naïve dermis at day 3 post infection, but by day 7 (which is the peak for the immigrant population), the  $CD103^-$   $\gamma\delta$  T cells produced Granzyme B. None of the  $\gamma\delta$  T cells in the dermis stained positive for IFN $\gamma$  at any time following VV scarification (Supplemental Figure 4C).

We repeated these intracellular staining experiments with BMpThy chimeras to determine whether the BM- and pThy-derived populations had distinct functions (Figure 4B). At day 3 post infection, there were too few BM-derived cells to be analyzed, but the pThy-derived  $\gamma\delta$  T cells readily produced IL-17. By day 7 post infection, a clear distinction between the two

populations could be seen, demonstrating that in this infection model, the function of adult BM-derived  $\gamma\delta$  T cells from the circulation was to make Granzyme B while the dermal pThy-derived  $\gamma\delta$  T cells gave rise to a population capable of making either IL-17 or, to a lesser extent, Granzyme B.

### Resident dermal $\gamma\delta$ T cells enhance the early immune response to infection

To determine whether  $\gamma\delta$  T cells contributed to inflammation and resolution of infection, we assessed tissue pathology and viral titers in wild type (WT) and  $\text{TCR}\delta^{-/-}$  mice, which lack all  $\gamma\delta$  T cells. By 3 days post infection, WT ears had evidence of both epidermal and cartilage necrosis, often with entire sections of the epidermis replaced by serocellular crusts (Figure 5A). The dermis of these mice predominantly contained accumulation of intact and degenerate neutrophils along with some macrophages and a fewer lymphocytes. In contrast, there was less infiltration of neutrophils and macrophages in the ears of  $\text{TCR}\delta^{-/-}$  mice and the cartilage and epidermis remained largely intact. Comparing the histological analysis for necrosis (combined for epidermis and cartilage) and cellularity, WT mice scored significantly higher than  $\text{TCR}\delta^{-/-}$  mice (Figure 5B). By day 7 post infection both groups had similar pathology (data not shown) and there was no difference in viral load between the ears of WT and  $\text{TCR}\delta^{-/-}$  mice over the course of infection either by PFU assay (Figure 5C) or by qPCR (data not shown).

We next compared histologic changes of BMpThy chimeras and BM chimeras to determine whether the differences between WT and  $\text{TCR}\delta^{-/-}$  mice could be assigned to the presence or absence of resident dermal  $\gamma\delta$  T cells. By and large, the BMpThy chimeras recreated the picture seen in WT mice with high scores for necrosis and cellularity. However, the BM chimeras had mild neutrophil infiltration, little to no cartilage necrosis and rare epidermal necrosis (Figure 5D & E). It was striking to see that replacement of dermal  $\gamma\delta$  T cells in BMpThy mice recapitulated results obtained with the WT mice and similarly, that BM mice mirrored  $\gamma\delta$  T cell null mice (Figure 5F). Thus, the loss of the dermal  $\text{CD}103^+$   $\gamma\delta$  T cell population appears sufficient to reduce ear inflammation and damage.

## DISCUSSION

Scarification of the skin with VV was used as a vaccine to eradicate small pox infection and the virus is now appreciated as an important vector for vaccine development and potentially cancer treatment (41). We have employed VV scarification of mouse ears to interrogate the distinct roles of recruited and resident dermal  $\gamma\delta$  T cells and to better understand their diversity. In this study, we describe for the first time the expansion, recruitment and contraction of  $\gamma\delta$  T cells in the dermis following localized VV infection. About half of the expanded dermal  $\gamma\delta$  T cells at day 7 were comprised of a unique population of  $\text{CD}103^- \text{CCR}6^-$   $\gamma\delta$  T cells that rapidly appeared in the dermis in response to infection. This novel population was derived primarily from circulating  $\text{CD}27^+$   $\gamma\delta$  T cells. A portion of the immigrant  $\gamma\delta$  T cells were phenotypically similar to the  $\text{CD}103^+$  IL-17 producing dermal-resident  $\gamma\delta$  T cell population and derived from circulating  $\text{CD}27^-$   $\gamma\delta$  T cells, although some were also found in the  $\text{CD}103^-$  fraction. These immigrant populations were functionally



distinct and played a discrete role from the resident dermal population, which was ultimately responsible for driving increased cellularity and tissue damage at an early time-point.

The number of dermal  $\gamma\delta$  T cells increased approximately 10-fold following VV infection and our data suggests that the majority of this increase can be ascribed to immigration rather than expansion of the resident population. Thus  $7 \times 10^5$  adoptively transferred  $\gamma\delta$  T cells made up 5% of the total  $\gamma\delta$  T cell population in the spleen and LNs before infection (data not shown) and this donor:host  $\gamma\delta$  T cells ratio was maintained in the dermis at day 7 following infection. Furthermore, the CD103/CCR6 profile of the adoptively transferred immigrants resembled that of the host  $\gamma\delta$  T cells in the dermis day 7 post-infection (Figure 2C), suggesting that not only is the entire CD103<sup>-</sup> population recruited, but many of the CD103<sup>+</sup>  $\gamma\delta$  T cells in the dermis may be as well. This in combination with the fact that we found very little in situ proliferation (Supplemental Figure 2) leads us to conclude that the accumulation of  $\gamma\delta$  T cells in the dermis is primarily due to recruitment.

The ability of immigrant cells to diversify into all the dermal subsets lead us to ask what the contribution was of the individual populations in the circulation. Emerging evidence confirms that CD27 delineates functional  $\gamma\delta$  T cell subsets in both mice (11, 29, 30) and humans (31–33). Transfer of CD27<sup>+</sup> and CD27<sup>-</sup> circulating  $\gamma\delta$  T cells into separate hosts followed by VV scarification demonstrated their unique contribution to CD103<sup>-</sup> or CD103<sup>+</sup> dermal populations, respectively. These experiments also confirmed the independent maintenance of these two populations even in the presence of inflammation. The stability of these two subsets and the constancy of the CCR6<sup>+</sup> and CCR6<sup>-</sup> ratio within the CD27<sup>-</sup> population offer an important tool for studying  $\gamma\delta$  T cells during inflammation. Although other groups have compared CD27<sup>+</sup> and CCR6<sup>+</sup>  $\gamma\delta$  T cells (11, 29), the circulating CCR6<sup>-</sup>CD27<sup>-</sup> subset has received less attention. This latter population is uniformly ROR $\gamma$ t<sup>+</sup> and distinguished from the CCR6<sup>+</sup> population by lower levels of CD103 and CD44 (Supplemental Figure 1A). Future studies will be needed to explore the nuances between these populations.

Although there is some disagreement concerning the radiosensitivity of  $\gamma\delta$  T cells and their reconstitution in an irradiated adult mouse (11, 16, 22), our chimera experiments revealed that, unlike the DETC population,  $\gamma\delta$  T cells in the circulation and dermis are radiosensitive. Our results confirm that transfer of perinatal thymocytes into an irradiated host generates bonafide CCR6<sup>+</sup>CD27<sup>-</sup>  $\gamma\delta$  T cells in the circulation and residents in the dermis. Differential kinetics and functional profiles of the BM (immigrant) and pThy (resident)  $\gamma\delta$  T cell populations in the BMpThy chimeras allowed us to ask whether they had distinct roles following infection. Determining the role of dermal  $\gamma\delta$  T cells by comparing WT and TCR $\delta$ <sup>-/-</sup> mice is complicated by the absence of normal DETC in the null mice (14), cells that are known to play a role in keratinocyte growth and survival, perhaps impacting tissue damage or recovery. Whole body irradiation allowed us to specifically deplete the resident dermal  $\gamma\delta$  T cells, creating mice that lack this population while retaining healthy BM-derived circulating  $\gamma\delta$  T cell populations. Comparing mice specifically with or without dermal  $\gamma\delta$  T cells revealed that the dermal resident population was responsible for the increased inflammation observed in infected WT animals (Figure 5D & E).

The ability of pThy-derived dermal  $\gamma\delta$  T cells to recruit inflammatory cells, such as neutrophils, is likely due to their production of IL-17 (16, 20, 42) and recruitment of neutrophils by  $\gamma\delta$  T cells directly results in increased tissue damage (43). We demonstrated increased necrosis and cellularity of infected ears 3 days after VV infection, indicating that the resident IL-17<sup>+</sup>  $\gamma\delta$  T cells are early responders to viral infection. In contrast, the immigrating population of CD103<sup>-</sup>CCR6<sup>-</sup> DN  $\gamma\delta$  T cells, which appeared concurrently, only upregulated Granzyme B expression at a later time-point. Although classically associated with cytotoxicity, which has been shown for  $\gamma\delta$  T cells (44), Granzyme B has direct antiviral effects within cells and can cleave structural proteins when released into the extracellular matrix (45, 46). Importantly for our study, extracellular Granzyme B release has been shown to have remodeling activity (47), potentially facilitating migration of cells into the tissue and impacting wound repair. Considering the absence of  $\gamma\delta$  T cells had no effect on viral load (Figure 5C) and the number of  $\gamma\delta$  T cells within the dermis remained elevated for an extended period of time, these Granzyme-producing cells may play a non-traditional role during inflammation and in the recovery process after viral clearance.

Little is known about whether  $\gamma\delta$  T cells can form 'memory'. The majority of studies have examined at total  $\gamma\delta$  T cell population re-expansion (48, 49) or relied on CD44 expression (33), which is now appreciated to be regulated differently in  $\gamma\delta$  T cells than classical  $\alpha\beta$  T cells (50). When we transferred congenically marked  $\gamma\delta$  T cells, none of the immigrant  $\gamma\delta$  T cells remained in the dermis as residents after infection was cleared (Figure 2B). This was true for the CD27<sup>+</sup> circulating  $\gamma\delta$  T cells characterized as CD103<sup>-</sup>CCR6<sup>-</sup> DN cells in the dermis and for the CD27<sup>-</sup> circulating cells that give rise to all three populations in the dermis at day 7 post infection. Similarly in the BMpThy chimeras, BM-derived circulating  $\gamma\delta$  T cells that entered during the infection did not remain there long term (Figure 3D). This indicates that inflammation is not sufficient to drive the long-term skin residence of  $\gamma\delta$  T cells that enter the skin from the circulation. In contrast, it has been observed after oral *Listeria monocytogenes* infection that a population of  $\gamma\delta$  T cells with memory-like function develop and persist in intestinal tissues (51). However, generating resident dermal  $\gamma\delta$  T cells requires a neonatal population (or their precursors), derived in our case from the transfer of perinatal thymocytes into irradiated hosts.

The presence of pThy-derived  $\gamma\delta$  T cells in the dermis was required to increase cellularity near the site of infection and to amplify the overall potency of the immune response as demonstrated by increased tissue damage in WT and BMpThy mice. While the complete absence of  $\gamma\delta$  T cells did not translate to increased viral load in this or related systems (52, 53), other models have shown that mice lacking  $\gamma\delta$  T cells are more susceptible to bacterial infection (54) and have a decreased capacity for wound healing (13). Together, the data indicate that  $\gamma\delta$  T cells are a dynamic population with a range of functions, but that they might not respond equally to all inflammatory cues. Importantly, since there is no DETC counterpart in human skin (55), it has become increasingly important to isolate the relevance of  $\gamma\delta$  T cells in the dermis in models relevant to human disease. Our study employing the adoptive transfer of circulating  $\gamma\delta$  T cells into normal hosts and the creation of chimeras specifically lacking a dermal resident population will be useful for interrogating  $\gamma\delta$  T cell subsets and furthering our understanding of the dermal immune network.

## Supplementary Material

Refer to Web version on PubMed Central for supplementary material.

## ACKNOWLEDGEMENTS

We thank the University of Washington Histology and Imaging Core for preparation of histological sections, Dr. E. Gray for critical discussion and technical advice, and Dr. P. Fink for review of the manuscript. We also thank Dr. J. Turner (U of Chicago) for the TCR $\delta$ -H2BeGFP mice originally derived by I. Prinz (MH-Hannover).

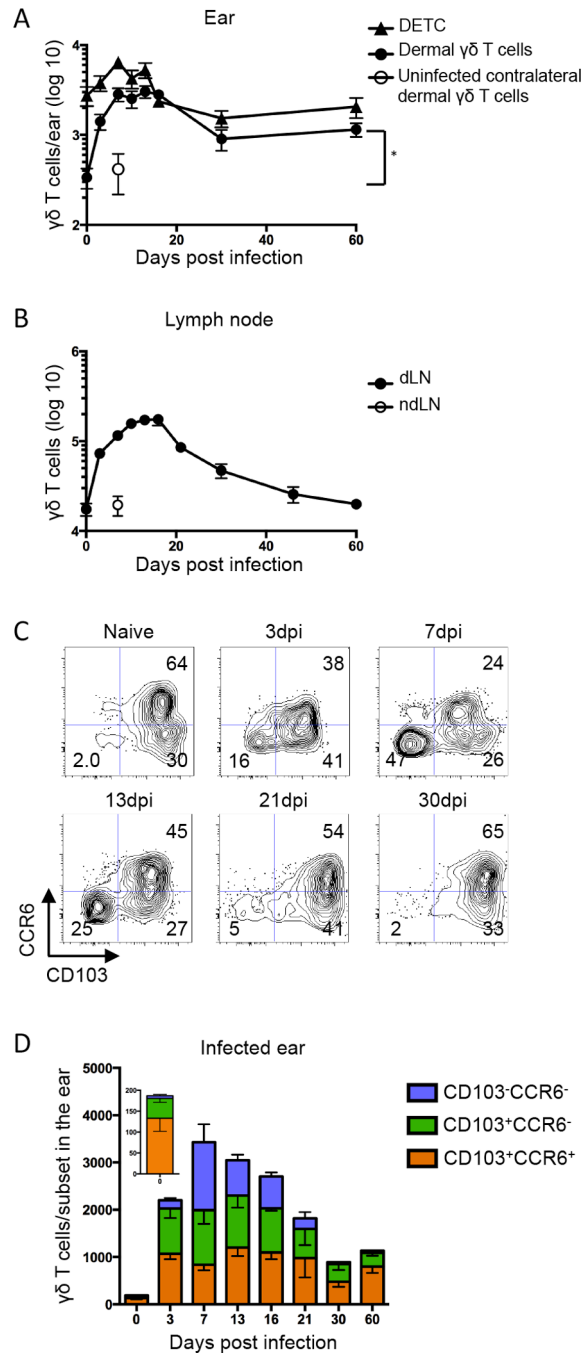
## REFERENCES

1. Heath WR, Carbone FR. The skin-resident and migratory immune system in steady state and memory: innate lymphocytes, dendritic cells and T cells. *Nat. Immunol.* 2013; 14:978–985. [PubMed: 24048119]
2. Tong PL, Roediger B, Kolesnikoff N, Biro M, Tay SS, Jain R, Shaw LE, Grimbaldston MA, Weninger W. The Skin Immune Atlas: Three-dimensional analysis of cutaneous leukocyte subsets by multiphoton microscopy. *J. Invest. Dermatol.* 2014
3. Zaid A, Mackay LK, Rahimpour A, Braun A, Veldhoen M, Carbone FR, Manton JH, Heath WR, Mueller SN. Persistence of skin-resident memory T cells within an epidermal niche. *Proc. Natl. Acad. Sci. U.S.A.* 2014; 111:5307–5312. [PubMed: 24706879]
4. Wakim LM, Gupta N, Mintern JD, Villadangos JA. Enhanced survival of lung tissue-resident memory CD8<sup>+</sup> T cells during infection with influenza virus due to selective expression of IFITM3. *Nat. Immunol.* 2013; 3:238–245. [PubMed: 23354485]
5. Wakim LM, Woodward-Davis A, Bevan MJ. Memory T cells persisting within the brain after local infection show functional adaptations to their tissue of residence. *Proc. Natl. Acad. Sci. U.S.A.* 2010; 107:17872–17879. [PubMed: 20923878]
6. Gebhardt T, Wakim LM, Eidsmo L, Reading PC, Heath WR, Carbone FR. Memory T cells in nonlymphoid tissue that provide enhanced local immunity during infection with herpes simplex virus. *Nat. Immunol.* 2009; 10:524–530. [PubMed: 19305395]
7. Mackay LK, Stock AT, Ma JZ, Jones CM, Kent SJ, Mueller SN, Heath WR, Carbone FR, Gebhardt T. Long-lived epithelial immunity by tissue-resident memory T (TRM) cells in the absence of persisting local antigen presentation. *Proc. Natl. Acad. Sci. U.S.A.* 2012; 109:7037–7042. [PubMed: 22509047]
8. Jiang X, Clark RA, Liu L, Wagers AJ, Fuhlbrigge RC, Kupper TS. Skin infection generates non-migratory memory CD8<sup>+</sup> TRM cells providing global skin immunity. *Nature.* 2012; 483:227–231. [PubMed: 22388819]
9. Shibata K. Close link between development and function of  $\gamma\delta$  T cells. *Microbiol. Immunol.* 2012; 56:217–227. [PubMed: 22300310]
10. Bandeira A, Mota-Santos T, Itohara S, Degermann S, Heusser C, Tonegawa S, Coutinho A. Localization of  $\gamma\delta$  T cells to the intestinal epithelium is independent of normal microbial colonization. *J. Exp. Med.* 1990; 172:239–244. [PubMed: 2141628]
11. Haas JD, Ravens S, Düber S, Sandrock I, Oberdörfer L, Kashani E, Chennupati V, Föhse L, Naumann R, Weiss S, Krueger A, Förster R, Prinz I. Development of Interleukin-17-producing  $\gamma\delta$  T cells is restricted to a functional embryonic wave. *Immunity.* 2012; 37:48–59. [PubMed: 22770884]
12. Allison JP, Havran WL. The immunobiology of T cells with invariant  $\gamma\delta$  antigen receptors. *Annu. Rev. Immunol.* 1991; 9:679–705. [PubMed: 1832874]
13. Havran WL, Jameson JM. Epidermal T cells and wound healing. *J. Immunol.* 2010; 184:5423–5428. [PubMed: 20483798]
14. Jameson JM, Cauvi G, Witherden DA, Havran WL. A keratinocyte-responsive  $\gamma\delta$  TCR is necessary for dendritic epidermal T cell activation by damaged keratinocytes and maintenance in the epidermis. *J. Infect. Dis.* 172:3573–3579.

15. Macleod AS, Havran WL. Functions of skin-resident  $\gamma\delta$  T cells. *Cell. Mol. Life. Sci.* 2011; 68:2399–2408. [PubMed: 21560071]
16. Sumaria N, Roediger B, Ng LG, Qin J, Pinto R, Cavanagh LL, Shklovskaya E, Fazekas de St Groth B, Triccas JA, Weninger W. Cutaneous immunosurveillance by self-renewing dermal  $\gamma\delta$  T cells. *J. Exp. Med.* 2011; 208:505–518. [PubMed: 21339323]
17. Holtmeier W, Pfander M, Hennemann A, Zollner TM, Kaufmann R, Caspary WF. The TCR $\delta$  repertoire in normal human skin is restricted and distinct from the TCR $\delta$  repertoire in the peripheral blood. *J. Invest. Dermatol.* 2001; 116:275–280. [PubMed: 11180004]
18. Maher BM, Mulcahy ME, Murphy AG, Wilk M, O'Keefe KM, Geoghegan JA, Lavelle EC, McLoughlin RM. Nlrp-3-driven Interleukin 17 production by  $\gamma\delta$  T cells controls infection outcomes during *Staphylococcus aureus* surgical site infection. *Infect. Immun.* 81:4478–4489. [PubMed: 24082072]
19. Byamba D, Kim DY, Kim D-S, Kim T-G, Jee H, Kim SH, Park T-Y, Yang S-H, Lee S-K, Lee M-G. Skin-penetrating methotrexate alleviates imiquimod-induced psoriasiform dermatitis via decreasing IL-17-producing  $\gamma\delta$  T cells. *Exp. Dermatol.* 2014; 23:492–496. [PubMed: 24824846]
20. Gray EE, Ramírez-Valle F, Xu Y, Wu S, Wu Z, Karjalainen KE, Cyster JG. Deficiency in IL-17-committed V $\gamma$ 4+  $\gamma\delta$  T cells in a spontaneous Sox13-mutant CD45.1+ congenic mouse substrain provides protection from dermatitis. *Nat. Immunol.* 2013; 14:584–592. [PubMed: 23624556]
21. Cai Y, Shen X, Ding C, Qi C, Li K, Li X, Jala VR, Zhang H-G, Wang T, Zheng J, Yan J. Pivotal role of dermal IL-17-producing  $\gamma\delta$  T cells in skin inflammation. *Immunity.* 2011; 35:596–610. [PubMed: 21982596]
22. Gray EE, Suzuki K, Cyster JG. Cutting Edge: Identification of a motile IL-17-producing  $\gamma\delta$  T cell population in the dermis. *J. Immunol.* 2011; 186:6091–6095. [PubMed: 21536803]
23. Haas JD, Gonzalez FHM, Schmitz S, Chennupati V, Föhse L, Kremmer E, Förster R, Prinz I. CCR6 and NK1.1 distinguish between IL-17A and IFN $\gamma$  producing  $\gamma\delta$  effector T cells. *Eur. J. Immunol.* 2009; 39:3488–3497. [PubMed: 19830744]
24. Maloy KJ, Odermatt B, Hengartner H, Zinkernagel RM. Interferon  $\gamma$ -producing  $\gamma\delta$  T cell-dependent antibody isotype switching in the absence of germinal center formation during virus infection. *Proc. Natl. Acad. Sci. U.S.A.* 1998; 95:1160–1165. [PubMed: 9448302]
25. Selin LK, Santolucito PA, Pinto AK, Szomolanyi-Tsuda E, Welsh RM. Innate immunity to viruses: control of vaccinia virus infection by  $\gamma\delta$  T cells. *J. Immunol.* 2001; 166:6784–6794. [PubMed: 11359837]
26. Mann ER, McCarthy NE, Peake STC, Milestone AN, Al-Hassi HO, Bernardo D, Tee CT, Landy J, Pitcher MC, Cochrane SA, Hart AL, Stagg AJ, Knight SC. Skin- and gut-homing molecules on human circulating  $\gamma\delta$  T cells and their dysregulation in inflammatory bowel disease. *Immunology.* 2012; 170:122–130.
27. Argentati K, Re F, Serresi S, Tucci MG, Bartozzi B, Bernardini G, Provinciali M. Reduced number and impaired function of circulating  $\gamma\delta$  T cells in patients with cutaneous primary melanoma. *J. Invest. Dermatol.* 2003; 120:829–834. [PubMed: 12713589]
28. Laggner U, Di Meglio P, Perera GK, Hundhausen C, Lacy KE, Ali N, Smith CH, Hayday AC, Nickoloff BJ, Nestle FO. Identification of a novel proinflammatory human skin-homing V $\gamma$ 9V $\delta$ 2 T cell subset with a potential role in psoriasis. *J. Infect. Dis.* 187:2783–2793.
29. Schmolka N, Serre K, Grosso AR, Rei M, Pennington DJ, Gomes AQ, Silva-Santos B. Epigenetic and transcriptional signatures of stable versus plastic differentiation of proinflammatory  $\gamma\delta$  T cell subsets. *Nat. Immunol.* 2013; 14:1093–1100. [PubMed: 23995235]
30. Ribot JC, deBarros A, Pang DJ, Neves JF, Peperzak V, Roberts SJ, Girardi M, Borst J, Hayday AC, Pennington DJ, Silva-Santos B. CD27 is a thymic determinant of the balance between interferon- $\gamma$ - and interleukin 17-producing  $\gamma\delta$  T cell subsets. *Nat. Immunol.* 2009; 10:427–436. [PubMed: 19270712]
31. deBarros A, Chaves-Ferreira M, d'Orey F, Ribot JC, Silva-Santos B. CD70-CD27 interactions provide survival and proliferative signals that regulate T cell receptor-driven activation of human  $\gamma\delta$  peripheral blood lymphocytes. *Eur. J. Immunol.* 2010; 41:195–201. [PubMed: 21182090]

32. Caccamo N, La Mendola C, Orlando V, Meraviglia S, Todaro M, Stassi G, Sireci G, Fournie JJ, Dieli F. Differentiation, phenotype, and function of interleukin-17-producing human V $\gamma$ 9V $\delta$ 2 T cells. *Blood*. 2011; 118:129–138. [PubMed: 21505189]
33. Dieli F, Poccia F, Lipp M, Sireci G, Caccamo N, Di Sano C, Salerno A. Differentiation of effector/memory V $\delta$ 2 T cells and migratory routes in lymph nodes or inflammatory sites. *J. Exp. Med*. 2003; 198:391–397. [PubMed: 12900516]
34. Wang T, Scully E, Yin Z, Kim JH, Wang S, Yan J, Mamula M, Anderson JF, Craft J, Fikrig E. IFN- $\gamma$ -producing  $\gamma\delta$  T cells help control murine West Nile virus infection. *J. Immunol*. 2003; 171:2524–2531. [PubMed: 12928402]
35. Pennington DJ, Silva-Santos B, Shires J, Theodoridis E, Pollitt C, Wise EL, Tigelaar RE, Owen MJ, Hayday AC. The inter-relatedness and interdependence of mouse T cell receptor  $\gamma\delta$ + and  $\alpha\beta$ + cells. *Nat. Immunol*. 2003; 4:991–998. [PubMed: 14502287]
36. Prinz I, Sansoni A, Kissenpennig A, Ardouin L, Malissen M, Malissen B. Visualization of the earliest steps of  $\gamma\delta$  T cell development in the adult thymus. *Nat. Immunol*. 2006; 7:995–1003. [PubMed: 16878135]
37. Liu L, Fuhlbrigge RC, Karibian K, Tian T, Kupper TS. Dynamic programming of CD8+ T cell trafficking after live viral immunization. *Immunity*. 2006; 25:511–520. [PubMed: 16973385]
38. Heilig JS, Tonegawa S. Diversity of murine gamma genes and expression in fetal and adult T lymphocytes. *Nat. Immunol*. 1986; 322:836–840.
39. Tschärke DC, Smith GL. A model for vaccinia virus pathogenesis and immunity based on intradermal injection of mouse ear pinnae. *J. Gen. Virol*. 80:2751–2755. [PubMed: 10573171]
40. Sutton CE, Lalor SJ, Sweeney CM, Breerton CF, Lavelle EC, Mills KHG. Interleukin-1 and IL-23 induce innate IL-17 production from  $\gamma\delta$  T cells, amplifying Th17 responses and autoimmunity. *Immunity*. 2009; 31:331–341. [PubMed: 19682929]
41. Veradi PH, Titong A, Hagen CJ. A vaccinia virus renaissance: new vaccine and immunotherapeutic uses after smallpox eradication. *Hu. Vac. Immuno*. 2012; 8:961–970.
42. Shibata K, Yamada H, Hara H, Kishihara K, Yoshikai Y. Resident V $\delta$ 1+  $\gamma\delta$  T cells control early infiltration of neutrophils after *Escherichia coli* infection via IL-17 production. *J. Immunol*. 2007; 178:4466–4472. [PubMed: 17372004]
43. Toth B, Alexander M, Daniel T, Chaudry IH, Hubbard WJ, Schwacha MG. The role of  $\gamma\delta$  T cells in the regulation of neutrophil-mediated tissue damage after thermal injury. *J. Leukoc. Biol*. 2004; 76:545–552. [PubMed: 15197233]
44. Qin G, Mao H, Zheng J, Sia SF, Liu Y, Chan PL, Lam K-T, Peiris JSM, Lau Y-L, Tu W. Phosphoantigen-expanded human  $\gamma\delta$  T cells display potent cytotoxicity against monocyte-derived macrophages infected with human and avian Influenza viruses. *J. Infect. Dis*. 2009; 200:858–865. [PubMed: 19656068]
45. Romero V, Andrade F. Non-apoptotic functions of granzymes. *Tissue Antigens*. 2008; 71:409–416. [PubMed: 18331532]
46. Andrade F. Non-cytotoxic antiviral activities of granzymes in the context of the immune antiviral state. *Immun. Rev*. 2010; 235:128–146. [PubMed: 20536560]
47. Buzza MS, Zamurs L, Sun J, Bird CH, Smith AI, Trapani JA, Froelich CJ, Nice EC, Bird PI. Extracellular Matrix Remodeling by Human Granzyme B via Cleavage of Vitronectin, Fibronectin, and Laminin. *J. Biol. Chem*. 280:23549–23558. [PubMed: 15843372]
48. Shen Y, Zhou D, Qiu L, Lai X, Simon M, Shen L, Kou Z, Wang Q, Jiang L, Estep J, Hunt R, Clagett M, Sehgal PK, Li Y, Zeng X, Morita CT, Brenner MB, Letvin NL, Chen ZW. Adaptive immune response of V $\gamma$ 2V $\delta$ 2+ T cells during mycobacterial infections. *Science*. 2002; 295:2255–2258. [PubMed: 11910108]
49. Shao L, Huang D, Wei H, Wang RC, Chen CY, Shen L, Zhang W, Jin J, Chen ZW. Expansion, reexpansion, and recall-like expansion of V $\gamma$ 2V $\delta$ 2 T cells in smallpox vaccination and monkeypox virus infection. *J. Virol*. 2009; 83:11959–11965. [PubMed: 19740988]
50. Wencker M, Turchinovich G, Di Marco Barros R, Deban L, Jandke A, Cope A, Hayday AC. Innate-like T cells straddle innate and adaptive immunity by altering antigen-receptor responsiveness. *Nat. Immunol*. 2013; 15:80–87. [PubMed: 24241693]

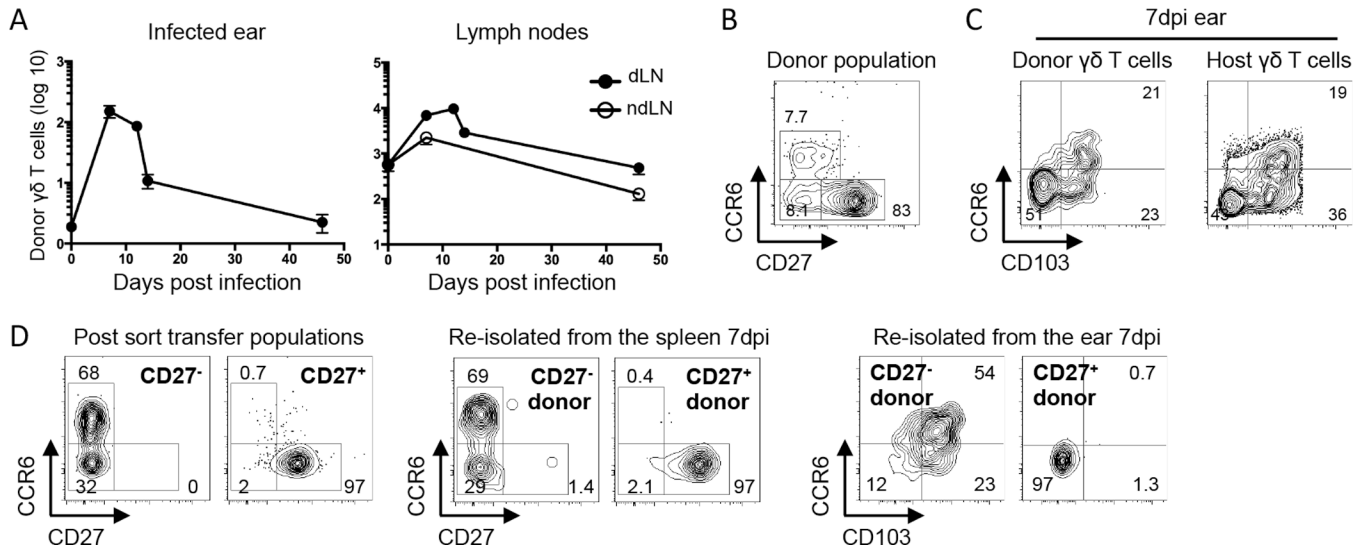
51. Sheridan BS, Romagnoli PA, Pham Q-M, Fu H-H, Alonzo F III, Schubert W-D, Freitag NE, LeFrancois L.  $\gamma\delta$  T cells exhibit multifunctional and protective memory in intestinal tissues. *Immunity*. 2013; 39:184–195. [PubMed: 23890071]
52. Kim J-O, Cha H-R, Kim E-D, Kweon M-N. Pathological effect of IL-17A-producing TCR $\gamma\delta$ + T cells in mouse genital mucosa against HSV-2 infection. *Immunol. Lett.* 2012; 147:34–40. [PubMed: 22698680]
53. McCarthy MK, Zhu L, Procario MC, Weinberg JB. IL-17 contributes to neutrophil recruitment but not to control of viral replication during acute mouse adenovirus type 1 respiratory infection. *Virology*. 2014; 456–457:259–267.
54. Hamada S, Umemura M, Shiono T, Tanaka K, Yahagi A, Begum MD, Oshiro K, Okamoto Y, Watanabe H, Kawakami K, Roark C, Born WK, O'Brien R, Ikuta K, Ishikawa H, Nakae S, Iwakura Y, Ohta T, Matsuzaki G. IL-17A produced by  $\gamma\delta$  T cells plays a critical role in innate immunity against *Listeria monocytogenes* infection in the liver. *J. Immunol.* 2008; 181:3456–3463. [PubMed: 18714018]
55. Elbe A. T-Cell receptor  $\alpha\beta$  and  $\gamma\delta$  T cells in rat and human skin — are they equivalent? *Semin. Immunol.* 1996; 8:341–349. [PubMed: 8961385]

**Figure 1.**

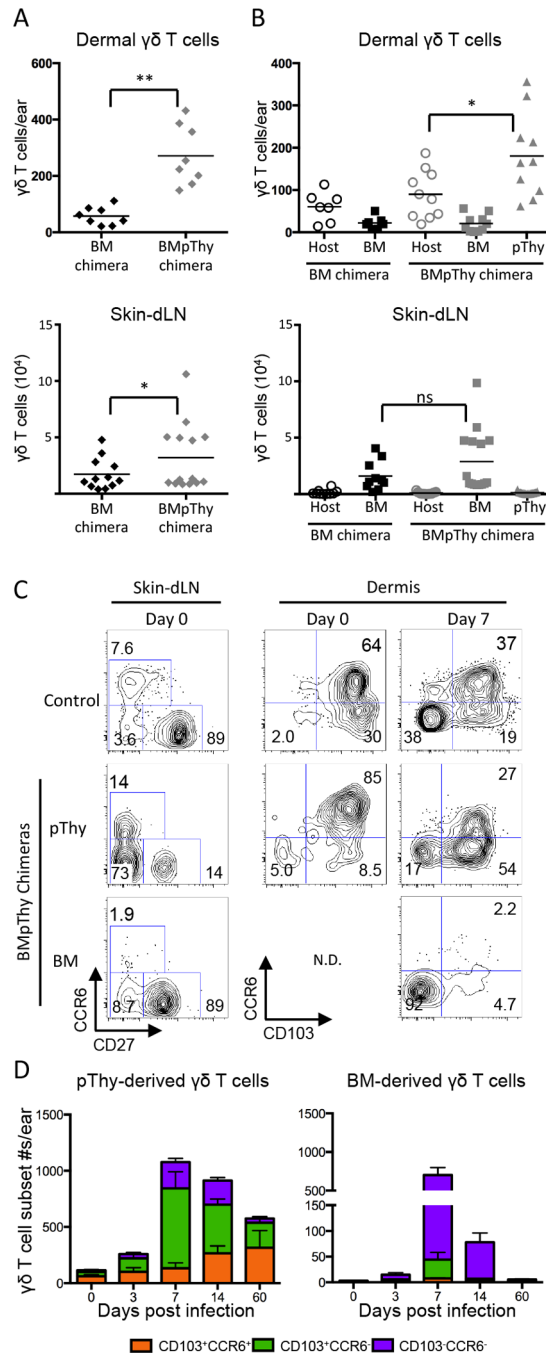
Following skin scarification with Vaccinia virus (VV),  $\gamma\delta$  T cells accumulate in draining lymph node and dermis. TCR $\delta$ -GFP mice were infected with VV on the ear by scarification.  $\gamma\delta$  T cells were gated as TCR $\beta$ <sup>-</sup>GFP<sup>+</sup> in the LN and as TCR $\beta$ <sup>-</sup>GFP<sup>+</sup>V $\gamma$ 5<sup>+</sup> (Dendritic Epidermal T Cells, DETC) or TCR $\beta$ <sup>-</sup>GFP<sup>+</sup>V $\gamma$ 5<sup>-</sup> (dermal  $\gamma\delta$  T cells) in the ear. A) Number of DETC and dermal  $\gamma\delta$  T cells in the ear following infection. Open symbol represents the number of dermal  $\gamma\delta$  T cells in the contralateral uninfected ear at 7dpi. B) Number of  $\gamma\delta$  T cells in the dLN following infection. Open symbol represents the number of  $\gamma\delta$  T cells in the

contralateral non-draining LN (ndLN) at 7dpi. C) Representative flow plots show CCR6 and CD103 profile of dermal  $\gamma\delta$  T cells following infection. Numbers denote percent of total dermal  $\gamma\delta$  T cell population within the indicated quadrant. D) Cell numbers within the indicated dermal  $\gamma\delta$  T cell subsets over the course of infection per ear (insert, day 0). Error bars signify SEM. Data are compiled from >5 (A, B) or >3 (C, D) independent experiments, n=3–13 mice per group. Statistics performed with the two-tailed, unpaired *t*-test, \**p*<0.001.



**Figure 2.**

Circulating  $\gamma\delta$  T cells migrate specifically to VV infected skin and contribute to all three dermal subsets. C57BL/6 mice (CD45.2) or CD45.2<sup>+</sup> TCR $\delta$ -GFP mice received  $7 \times 10^5$   $\gamma\delta$  T cells isolated from spleen and skin dLN of CD45.1<sup>+</sup> TCR $\delta$ -GFP mice. The following day, mice were infected with VV on the ear. A) Graphs show numbers of transferred TCR $\delta$ -GFP<sup>+</sup> cells recovered from the LN or ear, shown as  $\pm$  SEM. B) Representative flow plot shows the CCR6 and CD27 profile of the donor  $\gamma\delta$  T cell population prior to transfer. C) Representative flow plots show CCR6 and CD103 profile of donor and recipient dermal cells at 7dpi. D)  $\gamma\delta$  T cells from spleen and skin dLN of TCR $\delta$ -GFP mice were sorted based on CD27 expression and  $6 \times 10^5$  CD27<sup>+</sup> or  $2.7 \times 10^5$  CD27<sup>-</sup>  $\gamma\delta$  T cells were transferred into separate C57BL/6 hosts. Recipients were infected with VV on the ear the following day. Flow plots show the phenotype of CD27<sup>-</sup> and CD27<sup>+</sup> at the time of transfer and 7dpi in the spleen and ear. Numbers denote the percentage of cells within the indicated quadrant. Data are representative of at least two independent experiments, n=3–7 mice per group.

**Figure 3.**

Contribution of adult BM-derived and perinatal thymus-derived  $\gamma\delta$  T cells to the dermal response. CD45.2<sup>+</sup> TCR $\delta$ -GFP mice were irradiated and reconstituted with BM (BM only) or with BM plus pThy (BMpThy). A) Graphs show the total number of  $\gamma\delta$  T cells > 8 weeks following reconstitution in the dermis and skin dLN. Geometric mean is shown. B) Contribution of BM-derived and pThy-derived  $\gamma\delta$  T cells in the dermis and LN. Geometric mean is shown. C) and D) BMpThy chimeras were infected with VV on the ear > 8 weeks following reconstitution. C) CCR6 and CD27 profiles of  $\gamma\delta$  T cells in the skin dLN and

CCR6 and CD103 profiles of  $\gamma\delta$  T cells in the dermis at day 0 and 7dpi (N.D. = not done). Numbers denote the percentage of that population within the indicated quadrant. D) The number of BM- and pThy-derived  $\gamma\delta$  T cells contributing to subsets in the dermis following infection. Error bars signify SEM. Statistics performed with the two-tailed, unpaired student *t*-test, \**p*<0.02, \*\**p*<0.0001, NS = not significant. Data show results from >3 (A, B) or >2 independent experiments (C, D), n=3–15 mice per group.

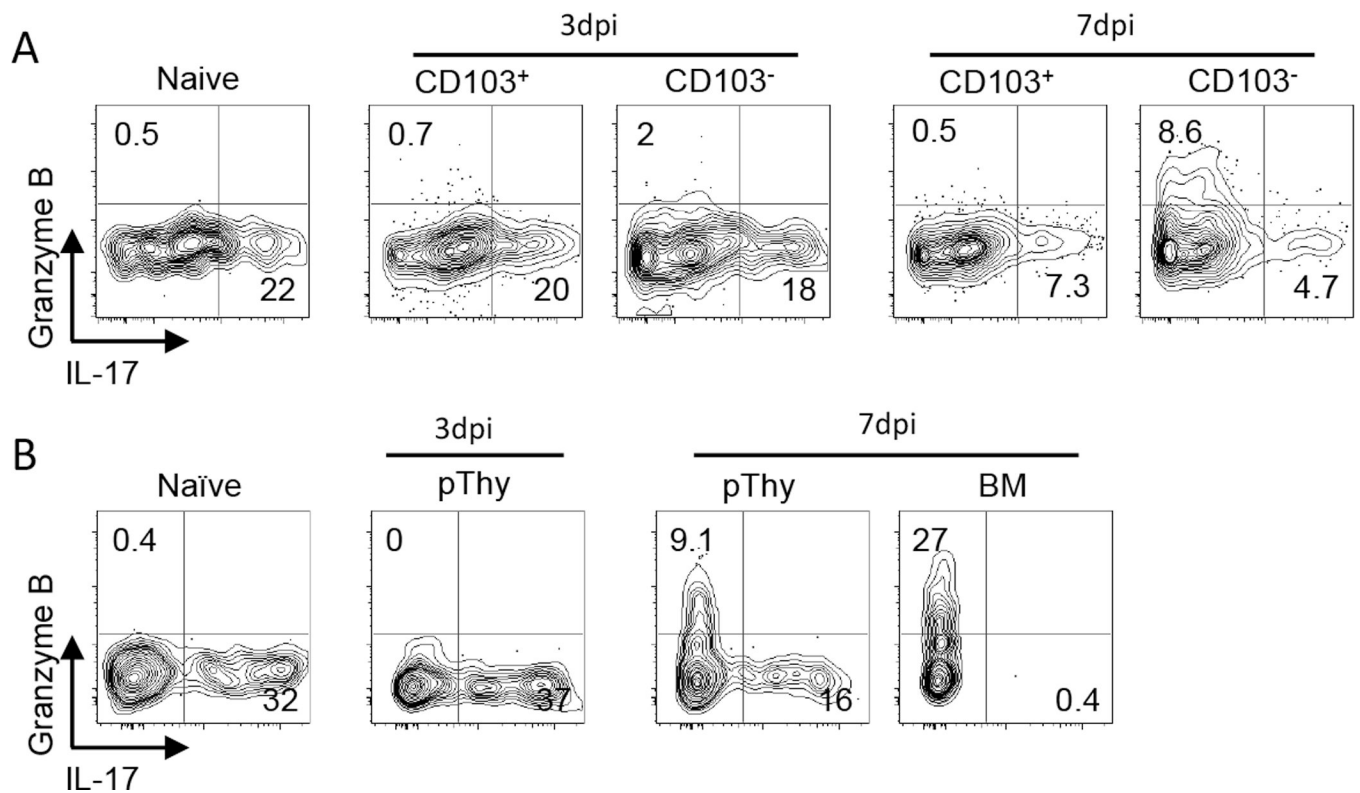


**Figure 4.** Adult BM-derived and pThy-derived  $\gamma\delta$  T cells in the dermis are functionally distinct. A) TCR $\delta$ -GFP mice and B) BMpThy chimeras were infected with VV on the ear and sacrificed on days 3 and 7. Ears were digested in Brefeldin A and cells were re-stimulated with PMA/Ionomycin for 4 hours at 37°C followed by intracellular staining for cytokines and Granzyme B. Representative flow plots are shown and gates are based on unstimulated naïve samples. Numbers indicate the percentage of that population in each quadrant. Data are representative of at >2 independent experiments.

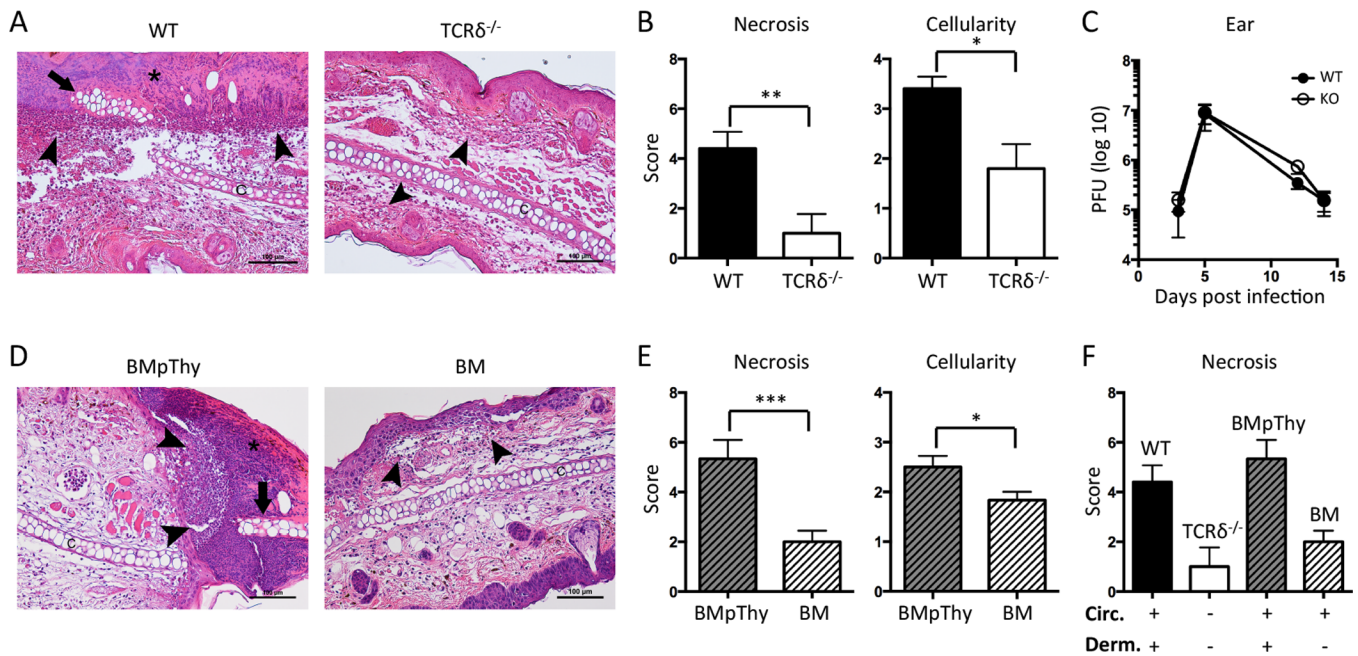


**Figure 5.** Dermal  $\gamma\delta$  T cells accelerate early collateral damage and contribute to increased tissue cellularity during VV infection. Mice were infected with VV on the ear. A) Representative histological sections of ears from C57BL/6 WT and TCR $\delta^{-/-}$  mice 3dpi at 20 $\times$  magnification. B) Graphs show scores for necrosis (epidermis and cartilage scored separately and then combined) and cellularity. Mean  $\pm$  SEM is shown. C) WT and TCR $\delta^{-/-}$  mice were sacrificed at the indicated time points following infection and ears were taken for plaque assay. Error bars indicate SEM. D) Representative histological sections and E) scores for BM chimeras and BMpThy chimeras 3dpi. Mean  $\pm$  SEM is shown. F) Comparison of necrosis scores for WT, TCR $\delta^{-/-}$ , BMpThy chimeras and BM chimeras in relation to the presence (+) or absence (-) of  $\gamma\delta$  T cell populations (Circ = circulating  $\gamma\delta$  T cells, Derm = dermal  $\gamma\delta$  T cells). Arrows indicate necrotic cartilage, arrowheads indicate neutrophilic infiltrates and asterisks indicate serocellular crusts. Statistics performed with the two-tailed, unpaired student *t*-test,  $n=5-6$  mice per group. \* $p<0.05$ , \*\* $p<0.01$ , \*\*\* $p<0.005$  Data are representative of  $>1$  independent experiments,  $n=3-6$  mice per group (C) or  $>2$  (A, B, D, E) independent experiments,  $n=5-6$  mice per group.